

Supplementary material

1. Seed laser characterisation

The performed experiments utilise three continuous wave (CW) ultra-narrow lasers (UNLs). We characterised the noise performance of the lasers utilising a commercially available self-homodyne noise measurement system. The input to the noise measurement system was fed by the 99% output of a coupler; the 1% tap fed an optical spectrum analyser (OSA) to record the central lasing wavelength. The central lasing wavelengths were obtained through Lorentzian fitting. The resolution bandwidth of the OSA traces were 40fm. All fibres and couplers utilised were polarisation maintaining angle-polished fibres. For all optical noise characterisations, single-sided noise data were obtained over a (100-100MHz) offset frequency range, with averaging over 200 traces, and a variable resolution bandwidth, per Table 1.

Offset frequency range (Hz)	Resolution bandwidth (Hz)
100-1k	3
1k-10k	30
10-100k	300
100k-1M	3k
1M-10M	5k
10M-100M	50k

Table 1: Utilised resolution bandwidths for each of the bands within the phase and relative intensity noise measurements.

Phase noise (PN), frequency noise (FN), and relative intensity noise (RIN) traces are provided in Fig. 1. The selected wavelengths for UNLs 1 and 2 lie in the centre of their respective tuning ranges. Root-mean-square (RMS) jitter, σ_ϕ , and fractional intensity fluctuations, σ_r , were calculated across the respective tuning ranges of UNLs 1 and 2. These are provided in Fig. 2a and 2b, respectively. The RMS jitter is taken from the phase noise data by integration of the phase noise over the Fourier (offset) frequency, Δf , where $(100 < \Delta f < 100M)$ Hz. The RMS jitter is calculated per

$$\sigma_\phi = \frac{1}{2\pi f_0} \sqrt{\int_{\Delta f_1}^{\Delta f_2} S_\phi(\Delta f) d\Delta f},$$

where f_0 is the central lasing frequency, taken from the curve fitting of the OSA trace.

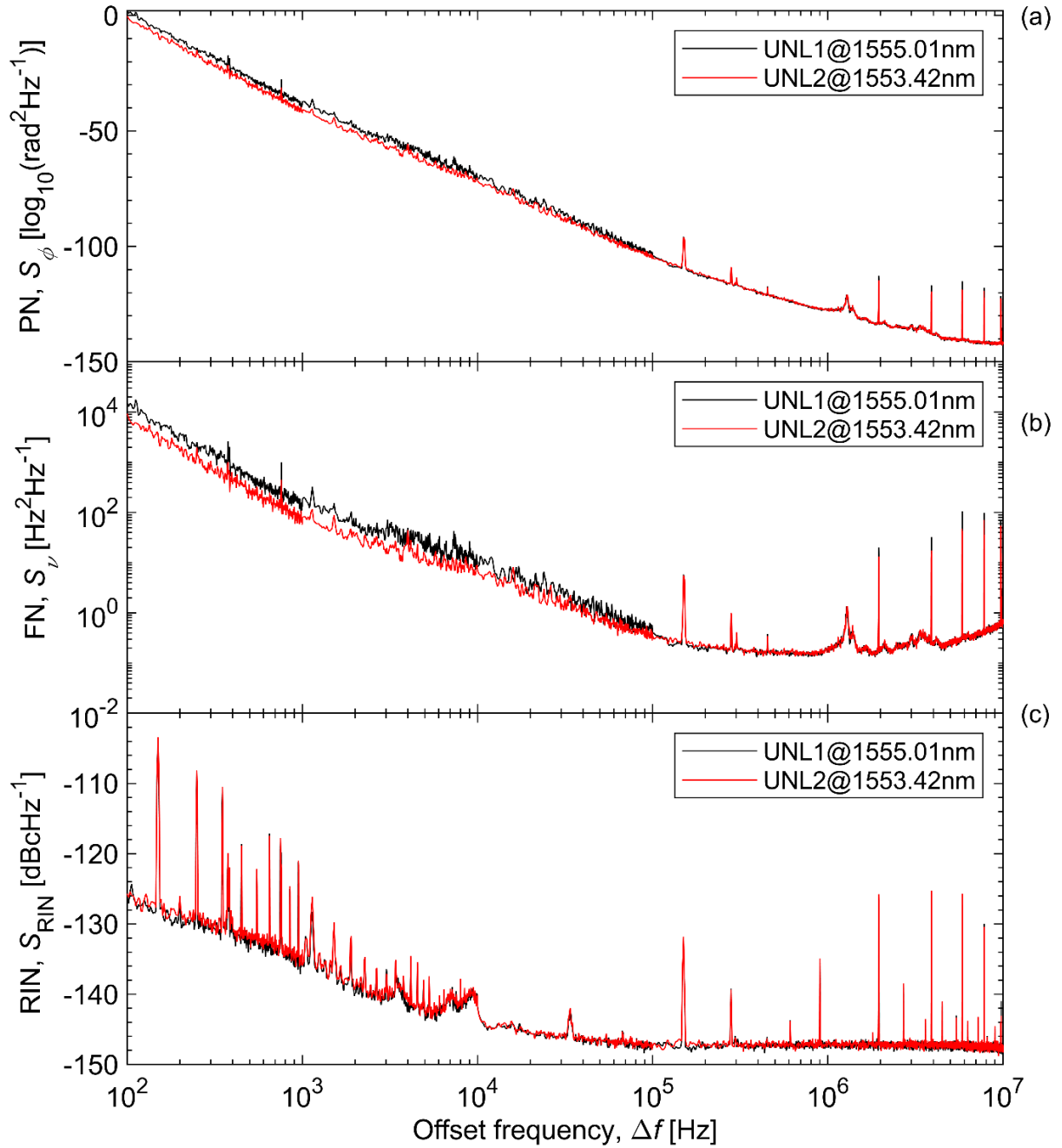


Figure S1: phase noise (a), frequency noise (b), and relative intensity noise (c) curves for the utilised UNLs. UNL1: OEwaves WGM laser with a fundamental linewidth of 40Hz. UNL2: OEwaves WGM laser with a fundamental linewidth of 7 Hz. The chosen wavelengths for the respective lasers were centred in their respective tuning ranges.

Similarly, the RMS fractional intensity fluctuations were calculated from the RIN data, again for varying wavelengths across the respective UNL tuning ranges, and by integrating over the Fourier frequency, per

$$\sigma_r = \sqrt{\int_{\Delta f_1}^{\Delta f_2} S_{\text{RIN}}(\Delta f) d\Delta f}.$$

For both RMS jitter and fractional intensity calculations, trapezoidal integrations were performed over the Fourier frequencies.

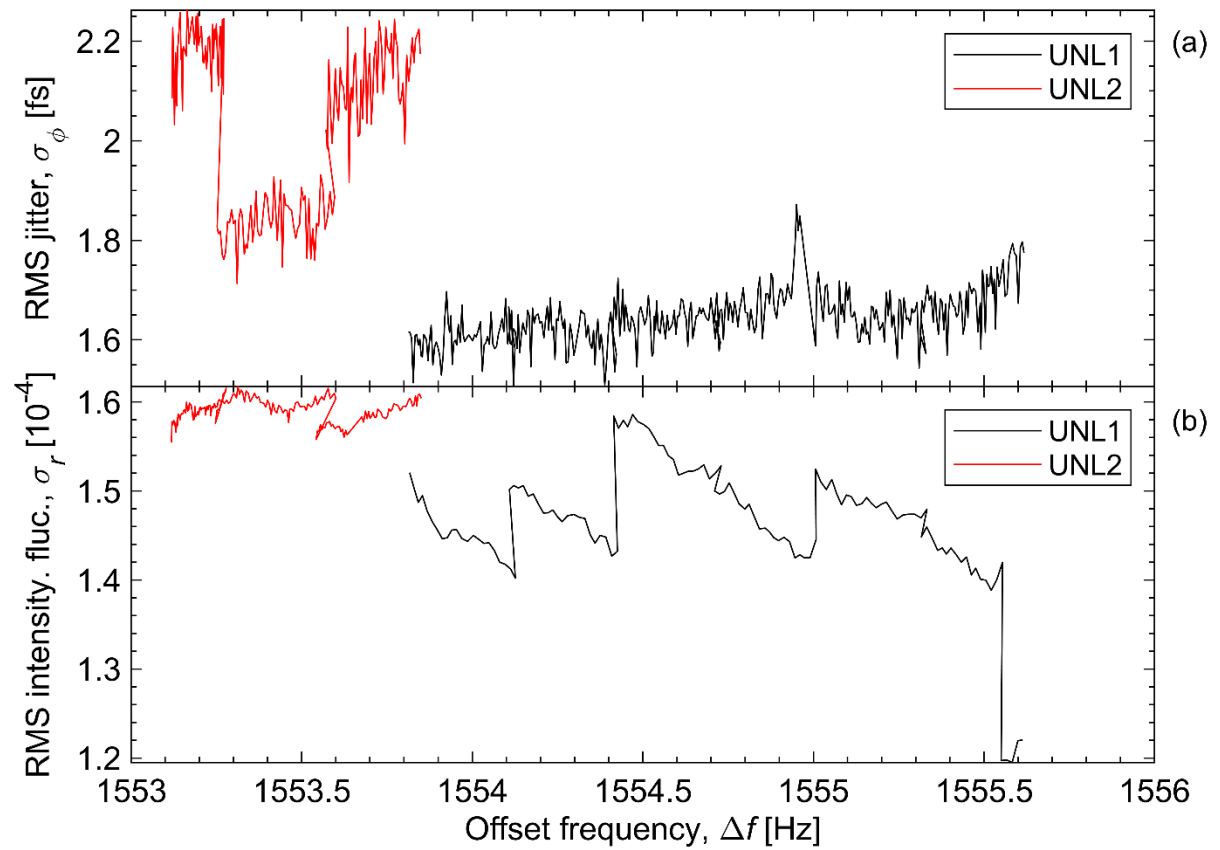


Figure S2: RMS jitter (a) and RMS intensity fractional fluctuation (b) curves for both UNLs across their respective tuning ranges.

2. RF Phase noise comparison of different synthesisers

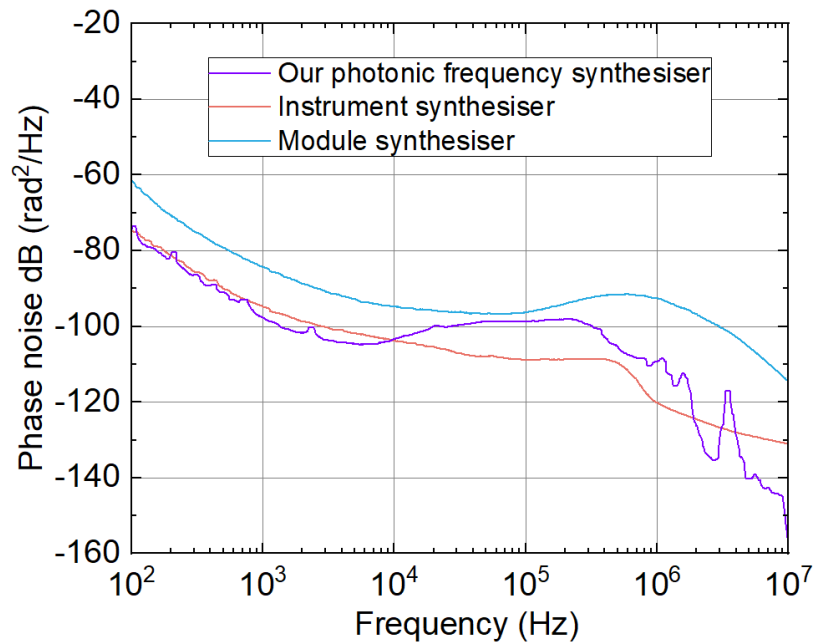


Fig. S3 Phase noise comparison of our photonic frequency synthesisers with instrument and module synthesisers

Fig. S3 shows the measured phase noise obtained using a phase noise analyser (Rohde & Schwarz FSWP). Phase noise was characterised using the cross-correlation method. The blue, purple, and pink traces correspond to the state-of-the-art module synthesiser, the proposed photonic frequency synthesiser, and instrument synthesiser (Rohde & Schwarz SMA100B with ultra-low noise option), respectively, all operating at 150 GHz. The measurement offset frequency range was configured from 100 Hz to 10 MHz.

From 100 Hz to 10 kHz, the photonic frequency synthesiser exhibits phase noise performance comparable to that of the instrument synthesiser. In the offset range from 10 kHz to 1 MHz, the SMA100B shows slightly lower phase noise, attributed to the limited locking bandwidth of the optical harmonic locking system. In contrast, the module synthesiser demonstrates inferior phase noise performance relative to the photonic frequency synthesiser across the entire measurement range.

3. 153GHz local oscillator generation using all-electronic synthesiser

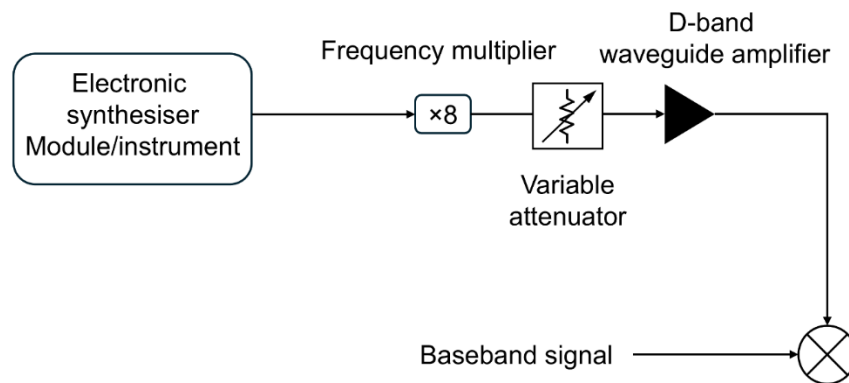


Fig. S4: 153GHz local oscillator generation using electronic synthesiser module/instrument

In the mm-wave signal transmission experiment, two electronics synthesisers (SignalCore SC5511A, Rohde&Schwarz SMA100B) are used to generate 19.125GHz signal with power of 7dBm, which is then fed into a frequency multiplier (Rohde & Schwarz SZM170, multiplication factor of 8), outputting 153GHz signal with 6dBm. The frequency multiplier output is connected to a D-band variable attenuator which attenuates the signal power to around -11dBm, followed by a D-band waveguide amplifier (VDI WR6.5AMP, 20dB gain) which boosts signal power to 10dBm. The input and output power of D-band amplifier is maintained same as photonic frequency synthesiser setup for fair comparison.

4. Frequency spectrum of down-converted D-band signal

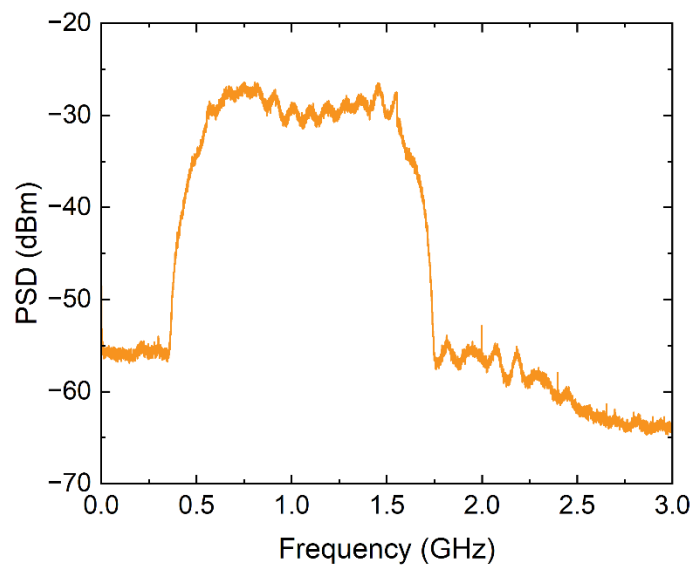


Fig. S5: Frequency spectrum of down-converted modulated D-band signal

In the mm-wave signal transmission experiment, the 153GHz-centred single-sideband signal was fed into a frequency down-converter (VDI WR6.5CCD). The down-converter has an integrated $\times 6$ frequency multiplication inside, which up-converts the input 24.65GHz local oscillator to 147.9GHz. By mixing input 153GHz-centred single-sideband signal with 147.9GHz carrier, the signal is down-converted to baseband. Fig. S5 shows the frequency spectrum of down-converted 64QAM signal at -16dBm received power, with resolution bandwidth of 1MHz. The ripple of spectrum is due to the frequency response of down-converter, fundamental mixer and D-band waveguide amplifier.